One-pot solvothermal method to prepare functionalized Fe_3O_4 nanoparticles for bioseparation

Guoxin Zhang[c)]
State Key Laboratory of Chemical Resource Engineering, Beijing University of Chemical Technology, Beijing, 100029, People's Republic of China

Fengxiang Qie,[c)] Jianxuan Hou, and Shizhong Luo
Beijing Key Lab of Bioprocess, College of Life Science and Technology, Beijing University of Chemical Technology, Beijing, 100029, People's Republic of China

Liang Luo and Xiaoming Sun[a)]
State Key Laboratory of Chemical Resource Engineering, Beijing University of Chemical Technology, Beijing, 100029, People's Republic of China

Tianwei Tan[b)]
Beijing Key Lab of Bioprocess, College of Life Science and Technology, Beijing University of Chemical Technology, Beijing, 100029, People's Republic of China

(Received 19 September 2011; accepted 23 January 2012)

Surface-functionalized magnetic nanoparticles were prepared by a facile one-pot solvothermal method in ethylene glycol solution. Zeta value, size, and magnetic properties could be well tuned by introducing different functional group molecules. Characterizations, including transmission electronic microscopy, scanning electronic microscopy, thermogravimetric analysis, x-ray powder diffraction and vibrating sample magnetometer, and Fourier transform infrared spectrophotometer demonstrated the efficiency of this simple and general synthesis strategy. The hydrophilic magnetic nanoparticles with various surface functional groups and zeta values were evidenced as excellent candidates for bioseparation by extracting DNA molecules from a model mixture of cell fractures.

I. INTRODUCTION

In recent years, magnetic iron oxide nanoparticles have received considerable attention for their superparamagnetic properties and low toxicity. Hydrophilic superparamagnetic iron oxide nanoparticles (HSPIONs) have attracted especial attention on account of their potential superiority for applications, such as bioseparations,[1–5] drug delivery,[6–9] cell imaging,[10–12] and magnetic resonance imaging (MRI).[13,14]

To date, HSPIONs could be formed by many technologies, such as coprecipitation,[15–17] microemulsion method,[18] sol–gel method,[19] thermal decomposition,[20,21] and solvothermal method.[22–25] The typical strategy involves iron oxide nanoparticles formation[26] and consequent post-synthesis surface modification or polymer encapsulation[15,27–29] to make the particles stable in aqueous phase and biocompatible.[22,24,30,31] Requirement of expensive and toxic initial materials, rigorous reaction conditions, low yield, time-consuming, and cost inefficiency might limit the scaling-up and applications of HSPIONs.

Very recently, Li's group made a breakthrough in this field by using ethylene glycol (EG) as both solvent and reducing agent for solvothermal synthesis of HSPION.[25] Morphology and crystallization of iron oxide nanomaterials could be easily tuned by this method.[32–36] More importantly, the method provided potentials for combining synthesis and surface functionalization in one step. For instance, amine modification was realized and used for detection and purification of biomolecules.[2,3,37–39] Potential applications include MRI,[10–14] drug carrier,[6–9] sensor,[40–42] and composite materials.[43]

Herein, we further developed the method by introducing various tuning reagents and systematically investigated the tailoring on surface potential and functional groups. A series of characterizations were implemented to gain deep view of our products. DNA isolation experiments were used to demonstrate the potential of the materials for bioseparation.

II. EXPERIMENTAL SECTION

A. Chemicals

The chemicals outlined below were of analytical purity, purchased from Beijing Chemical Reagent Factory (Beijing, China), and were used as-received without further purification unless otherwise noted.

Address all correspondence to these authors.
[a)]e-mail: sunxm@mail.buct.edu.cn
[b)]e-mail: twtan@mail.buct.edu.cn
[c)]These authors have contributed equally to this work.
DOI: 10.1557/jmr.2012.35

 © Materials Research Society 2012

https://doi.org/10.1557/jmr.2012.35 Published online by Cambridge University Press

B. Synthesis of surface-modified magnetic nanoparticles

In a typical synthesis for various organic group modified magnetic nanoparticles, 3.7 mmol ferric chloride ($FeCl_3 \cdot 6H_2O$, AR, ~1.00 g) was first added into 20 mL EG (AR) under ultrasonication at room temperature to form a clear solution; next, 2.42 mmol anhydrous sodium acetate (NaAc, AR, ~2.00 g) was poured into the mixture with magnetic stirring to form a uniform suspension, then 5 mL ethanediamine (EDA, AR)/1.00 g polyethyleneimine (PEI, AR, MW = 50,000, 50% solution, Aladdin)/1.50 g polyethylene glycol (PEG, AR, MW = 1000)/1.00 g sodium gluconate ("SG" in abbreviation, AR grade, Aladdin. Note: Dissolving SG in EG needs ultrasonication for >45 min.)/0.15 g polyacrylic acid (PAA, 60% solution, AR, MW = 2000, Aladdin) (Products were named respectively IO-EDA, IO-PEI, IO-PEG, IO-SG, and IO-PAA) were carefully added in the suspension. Finally, the solution was transferred into a 40 mL Teflon-sealed autoclave and reaction was maintained at 180–200 °C for 24 h.

For the synthesis of polyamidoamine (PAMAM)-modified magnetic nanoparticle, PAMAM was first synthesized followed Tomalia's method,[44] Michael addition reaction was used for the synthesis of the half generation.[45] In this addition reaction, a slight excess of methylacrylate (~10 mol%) was used for the alkylation step. Excess reagents and solvents were removed under vacuum (<1 mmHg) at a temperature of below 40 °C. 0.4 g $FeCl_2 \cdot 6H_2O$ was added into the vessel, and the coprecipitation method combined with solvothermal method was carried out with the reaction temperature at 180 °C (note: 200 °C would lead to decomposition of PAMAM). The black or puce products were isolated by outer magnet and rinsed by three cycles of centrifugation/washing/redispersion in water or alcohol, followed by oven-dried at 60 °C for more than 4 h.

C. Characterizations

1. Transmission electron microscopy measurement

The samples were first suspended in ethanol and then placed as the droplet onto a holey carbon-coated copper transmission electron microscopy (TEM) grid. Specimens were allowed to air-dry and imaged at 200 kV using a Hitachi H-800 (Tokyo, Japan).

2. Scanning electron microscope measurement

The samples were first suspended in ethanol and then placed onto a piece of silica wafer, which was treated with methanol, acetone, and isopropanol ordinally before used. Specimens were air-dried and imaged using a Zeiss SUPRA 55 (Oberkochen, Germany).

3. X-ray diffraction measurement

Powder x-ray diffraction (XRD) data were taken on a D/max-Ultima III (Rigaku, Tokyo, Japan) using Cu Kα radiation (40 kV, 30 mA, λ = 1.5418 Å). The samples, as unoriented powders, were step-scanned in steps of 0.02° (2θ) in the range 3–70° using a count time of 4 s per step.

4. Zeta potential measurements

Solid samples were ultrasonicated in deionized water for more than 10 min to form a transparent solution and measured by a Zetasizer instrument (ZS90 Malvern instruments, Worcestershire, UK) to define their surface charge properties.

5. Magnetic property measurements

The magnetization of the magnetic nanohybrid (Beijing, China) was tested on a JSM-13 vibrating sample magnetometer at 298 K and ± 15 kOe applied magnetic field.

6. Fourier transform infrared spectra analysis

The surface composition of the nanoparticles was studied by Fourier transform infrared (FTIR) spectroscopy with a Varian 3100 FTIR (Palo Alto, CA) in the 400–4000 cm^{-1} spectral range and a resolution of 2 cm^{-1}. The hydrophilic magnetic nanoparticles were mixed with KBr powder, then grounded and compacted into thin disk-shaped pellets. To avoid water molecule contamination, near-infrared lamp was used to dry the disk-shaped pellets.

7. Thermal analysis

The thermal analysis was conducted on a TA instruments (Thermo plus TG8120, Rigaku, Tokyo, Japan) in Ar gas with a heating rate of 10 °C/min from room temperature to 800 °C.

D. Test the capability of extracting nucleic acids

Surface-charged magnetic nanoparticles may take advantage of their surface potentials and plentiful functional groups for extracting biomolecules in various conditions. We chose nearly purified DNA (filtered from cell fracture in advance by Plasmid Maxi Kit from OMEGA, $A_{260\ nm}/A_{280\ nm} = 1.7223$) as the model target to separate. In a typical procedure, six kinds of magnetic particles were weighted separately (0.02 g each time after dryness) and washed with PBS buffer twice under assistance of ultrasonication and magnets. The supernatant was decanted. Model mixture was prepared by transforming plasmid into Escherichia coli and then cultivating and proliferation. Then 16 μL of 4.66 g/L model mixture ($A_{260\ nm}/A_{280\ nm} = 1.7223$)[46] containing DNA [ultraviolet–visible (UV–vis) absorption peak at 260 nm] and protein (UV–vis absorption peak at 280 nm) and 1.0 mL binding

https://doi.org/10.1557/jmr.2012.35 Published online by Cambridge University Press

buffer consisting of 20% PEG-8000 and 2 M NaCl were added into the microtube, the mixture was stirred for 15 min and kept still for 10 min. The supernatant was decanted after magnetic nanoparticles (MNPs) being drawn to the wall by magnet, the particles were washed twice using binding buffer and 70% ethanol, and the magnetic particles in the tube were dried at low temperature to remove excess ethanol. Finally, the DNA adsorbed on the magnetic particles was eluted by a common elution buffer: TE buffer (10 mM Tris-HCl, 1 mM ethylenediaminetetraacetic acid, and pH = 8.0). DNA quantification was realized by UV absorbance at 260 nm on a UV–vis Bio-Spectrophotometer (Varian CARY-100) and repeated for three times. The purity was determined on the basis of UV absorption ratio at 260–280 nm (A_{260}/A_{280}).

III. RESULTS AND DISCUSSION

Magnetite nanoparticles were formed by high-temperature hydrolysis of Fe^{3+} upon addition of NaAc in the presence of modificatory reagents. Under the reductive atmosphere provided by EG at high temperature, hydrolysis product, $Fe(OH)_3$, partially transforms to $Fe(OH)_2$ and finally multivalent magnetic iron oxide.[25] Here, typical positively charged organic molecules (EDA, PEI, and PAMAM) and typical negatively charged organic molecules (SG and PAA) were chosen to adjust the surface charge and type of functional groups.

A. XRD characterizations

The structure and phase purity of crystalline was determined by powder XRD, as shown in Fig. 1. The sharp, strong peaks confirmed the products were well crystallized. It can be seen that IO-EDA, IO-PEI, IO-PAMAM, IO-PEG, IO-SG, and IO-PAA presented typical reflections of face center cubic iron oxide (JCPDS no. 65-3107), which were indexed into the (220), (311), (400), (422), (511), and (440) peaks. Calculations with the Debye–Scherrer formula for the strongest peak (311) gave grain sizes of IO-EDA, IO-PEI, IO-PAMAM, IO-PEG, IO-SG, and IO-PAA for hydrophilic magnetic nanoparticles with sizes of 20.73, 19.01, 8.73, 21.77, 9.22, and 6.81 nm, respectively. The result implies that the primary nanocrystals do not grow significantly with increasing size of magnetic nanoparticles while the primary crystalline could be also tuned by those modifactory agents.

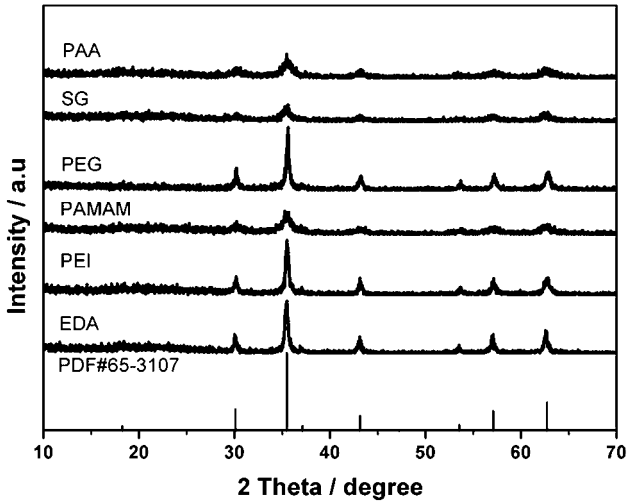


FIG. 1. X-ray diffraction patterns, marked by corresponding modified agents.

B. Size and morphology characterization

The size and shape of products were examined by TEM and scanning electron microscope (SEM). Figure 2 showed the typical TEM images of the as-prepared magnetite nanoparticles. The average diameter of the samples are between 100 and 200 nm. Former reports of magnetic nanoparticles synthesis showed that the size could be tuned by adjusting reaction temperature and time[12,22]: usually longer time and higher temperature would make bigger ones. Here, we introduced various tuning reagents to synthesize magnetic nanoparticles and investigated the effect of modifactory agents. Results indicated that the amount and type of modificatory reagents indeed affected the size of hydrothermal products, this may be due to the instinct of modifactory agents, crystals will certainly behave different under various conditions. SEM images of Fig. 3 coincided well with that of TEM images, which showed that surface morphology of six types of particles were coarse instead of smooth sphere, and they all had secondary structure consisting primary crystal in tens of nanometers, making them superparamagnetic. The properties of coarse surface and superparamagnetic may benefit bimolecular conjugation and bioseparation.

Dynamic light scattering (DLS) analysis (Fig. 4) gave the diameter around 200–300 nm for polymer (e.g., PEI, PEG, and PAA) wrapped IO nanoparticles, which fitted well with their TEM images. However, small molecules wrapped nanoparticles (IO-EDA and IO-SG) were about 1000 nm in diameter according to DLS results, which were attributed to aggregation in certain degree due to the relative weak repulsion induced by much thinner hydrated shell in comparison with magnetic attraction.

C. Surface properties characterization

Various organic molecules were introduced to increase the solubility of IO beads and tune the surface charge according to our requirements. We categorized these molecules into three kinds: basic (EDA, PEI, and PAMAM), neutral (PEG), and acidic (SG and PAA). The PEG had no active groups except of terminal hydroxyl groups. Since they are not readily binding to Fe^{2+} and Fe^{3+}, so the loading amount was limited [~3% showed by thermogravimetric analysis (TGA)], which surely cannot change much of

https://doi.org/10.1557/jmr.2012.35 Published online by Cambridge University Press

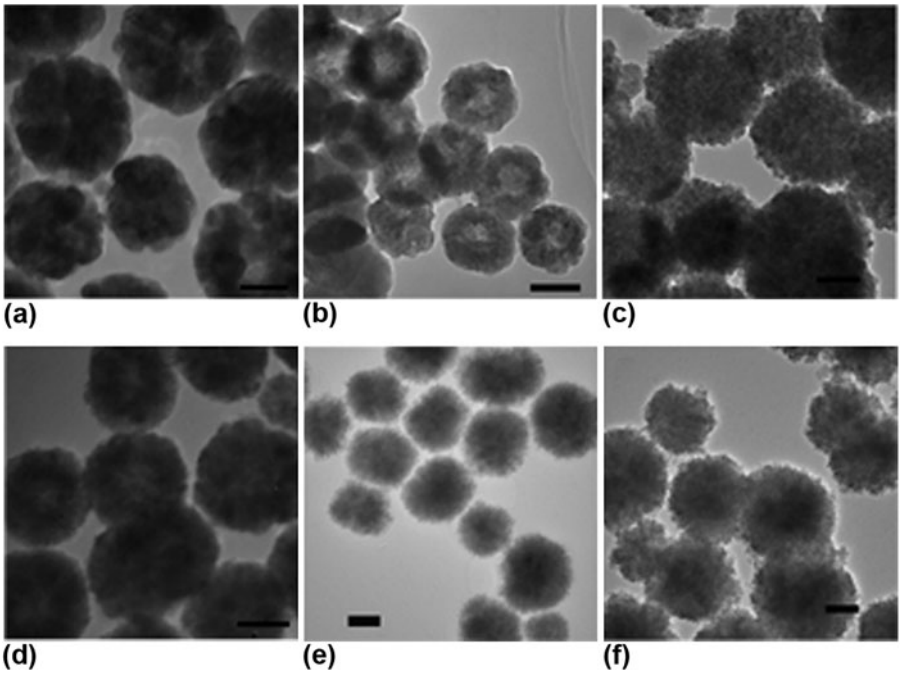


FIG. 2. Transmission electron microscopic images of (A) IO-EDA; (B) IO-PEI; (C) IO-PAMAM; (D) IO-PEG; (E) IO-SG; (F) IO-PAA. scale bar=100 nm.

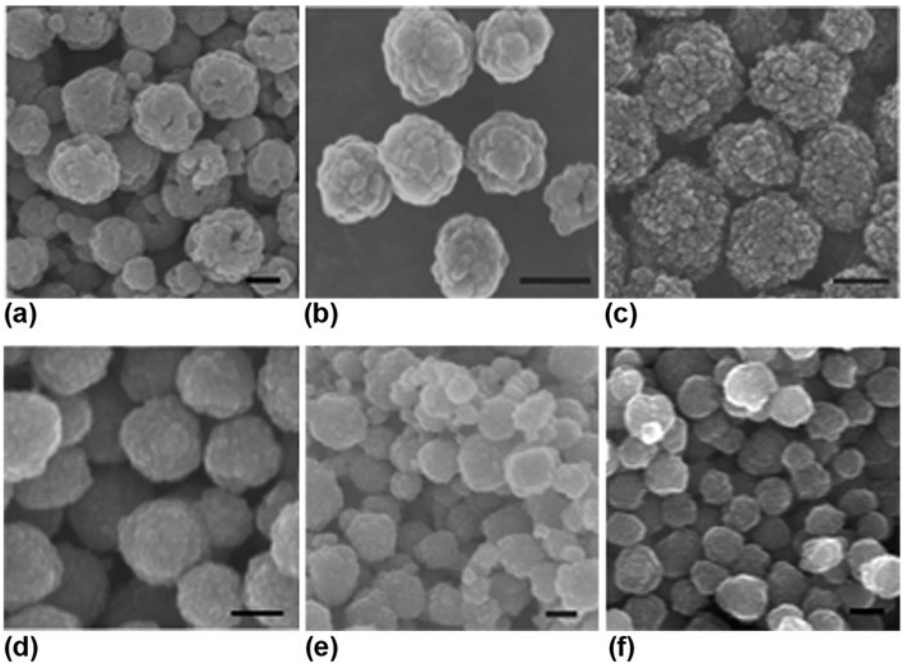


FIG. 3. Scanning electron microscopic images of (A) IO-EDA; (B) IO-PEI; (C) IO-PAMAM; (D) IO-PEG; (E) IO-SG; (F) IO-PAA. scale bar=100 nm.

surface charges. Basic molecules modification on IO beads will easily convert $-NH_2$ group into $-NH_3^+$ form, which endows positive charge on surface. On the contrary, acidic coating leads to negative charges by deprotonation. Surface properties were explored by zeta potential measurement and FTIR characterization. Zeta value graph (Fig. 5) showed that zeta values of IO-EDA, IO-PEI, IO-PAMAM, IO-PEG, IO-SG, and IO-PAA are 16.8, 47.6, 20.6, −14.8, −39.6, and −47.8 mV, respectively. It indicated that a wide range of zeta value of MNPs could be tuned by our one-pot solvothermal method. Surface functional groups determine the zeta value of magnetic nanoparticles: amine

https://doi.org/10.1557/jmr.2012.35 Published online by Cambridge University Press

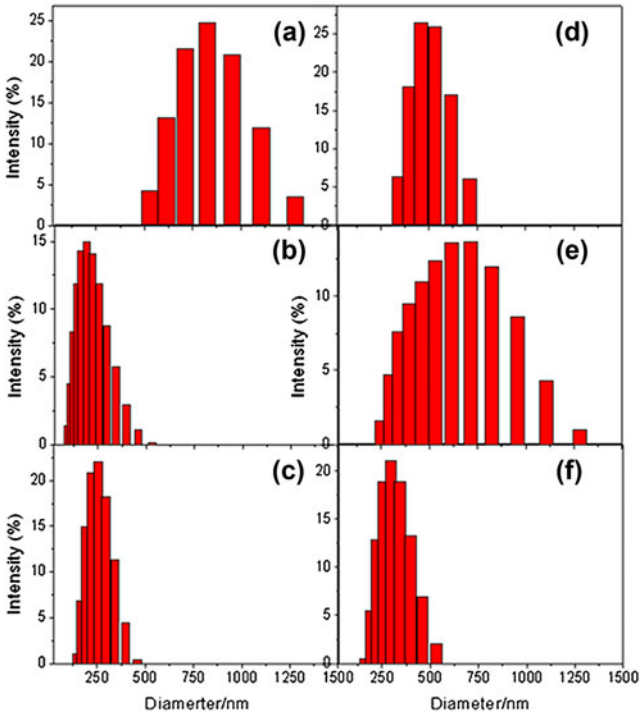


FIG. 4. Dynamic light scattering measurement of six kinds of magnetic nanoparticles. Respective Z-average diameter (nm): (A) IO-EDA, 1391.2; (B) IO-PEI, 190.9; (C) IO-PAMAM, 239.2; (D) IO-PEG, 468.8; (E) IO-SG, 816.9; (F) IO-PAA, 300.1.

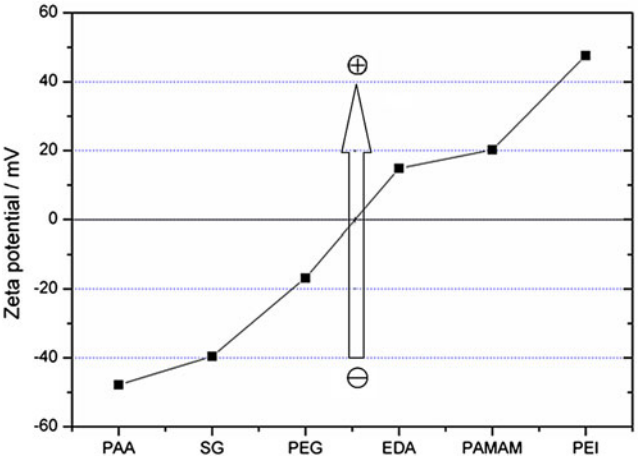


FIG. 5. Zeta potential analysis: surface charge properties could be tuned by different modifying agents.

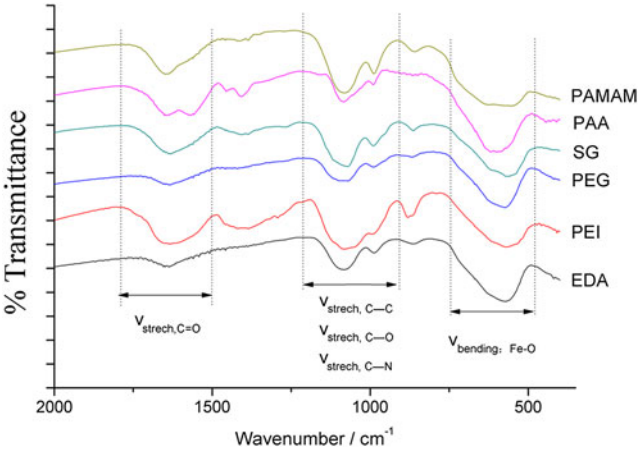


FIG. 6. Fourier transform infrared spectra of (A) IO-EDA; (B) IO-PEI; (C) IO-PAMAM; (D) IO-PEG; (E) IO-SG; (F) IO-PAA.

or amino-terminated PEI, EDA, and PAMAM render positive charges, while carbonate-terminated SG and PAA render negative charge, neutral surface functionalization using PEG inherit the weak negative charge state of crude magnetic nanoparticles. The surface functional groups could help to form stable suspension. We noticed that the small molecular EDA-modified magnetic nanoparticles precipitate in a few hours due to relatively thin hydrated shell and magnetic attraction.[22] But, long-chain macromolecule (e.g., PEG, PEI) modification extends the suspension stability by thickening the hydrated shell and/or strengthening the repulsive electrostatic force.

The IR spectroscope (Fig. 6) was used to reveal the existence of modificatory reagent on the six kinds of nanocrystalline surface. Three series of bands appears in common. Strong bands around 590 cm^{-1} are indexed to the Fe–O stretching modes of the magnetite for all samples.[47] A series of bands around 1000–1200 cm^{-1} corresponds to the stretching vibration of C–C and/or C–O bonds. Another common vibration locates around 1500–1750 cm^{-1}. For IO-PAA and IO-SG, it reveals the presence of carboxyl group (–C=O, at 1650 cm^{-1}), which reveals the loading of PAA and SG onto the MNPs. For other samples without carboxyl group (e.g., PEI), existence of vibrations at 1640 cm^{-1} is attributed to scissor vibration of $–CH_2–$. Weak –C–O–C– ether vibration band around 1400 cm^{-1} (antisymmetric stretch) indicates the partial esterification between SG molecules (Fig. 4). Band of 1150 cm^{-1} clearly shows the presence of C–N bond in the samples of IO-EDA, IO-PEI, and IO-PAMAM, implying the successful loading of organic layer.

D. Magnetic property

Better magnetic properties can benefit applications in applications like bioseparation or drug delivery. The hysteresis curves (Fig. 7) exhibited that the saturation magnetization of hydrophilic magnetic nanoparticles was between 42 and 82 emu/g, and the field dependence of the magnetization at 300 K showed low remanence (σ_r) and a very small coercivity (jHc $<$ 60 Oe), which indicated that six particles are all superparamagnetic. Values of some HSPIONs were comparable with those of Fe_3O_4 nanoparticles having macro- and nanosizes obtained by other aqueous approaches or with that of the bulk material (92 emu/g for magnetite),[48] which is strong enough for

https://doi.org/10.1557/jmr.2012.35 Published online by Cambridge University Press

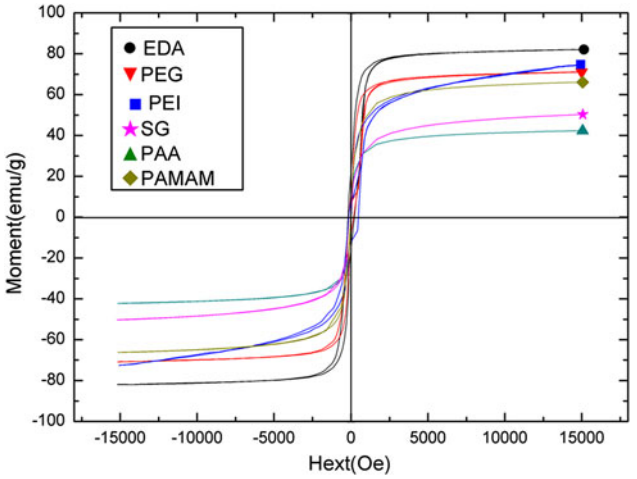


FIG. 7. Magnetization curves of six hydrophilic magnetic nanoparticles.

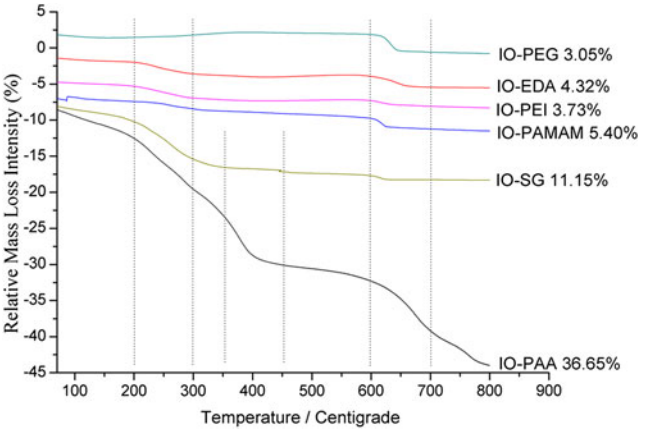


FIG. 8. Thermal deposition behavior under heating under inert gas (Ar). Relative mass loss intensities have been marked behind respective curves

bioseparation applications. Saturation magnetization of six products varied possibly due to the size dependence of magnetic nanoparticles and also amount difference of organic molecules on the surface.[24,30] Some studies suggested that the existence of surfactant or polymers on the surface of Fe_3O_4 nanoparticles quenched surface moments and reduced magnetic moment in such nanoparticles.[48]

E. TGA analysis

The TGA analysis (Fig. 8) was used to compare the organic molecule amounts on the magnetic iron oxide nanoparticles by showing different decomposition behavior in 100–700 °C. First, weight loss is observed between the temperatures of 50–110 °C which is due to the evaporation of physically adsorbed water on the surface of HSPIONs. Other two typical stages: one is 200–300 °C and the other is 600–700 °C. The former is attributed to the decomposition of modifactory reagents to NH_3 or CO_2 (formed by initially partial decomposition).[28,30] The latter was probably caused by carbothermic reduction to form α-Fe or γ-Fe.[49] Special weight loss of IO-SG and IO-PAA was spied at the range of 350 and 450 °C, it may be caused by loss of CO or CO_2 molecule formed by carbonization.[50]

F. Extracting DNA from model mixture

The functionalized magnetic particles are widely used in bioseparations through specific[22,30,51] and nonspecific molecular binding.[52,53] Here, we investigated the effects of surface modification for nonspecific DNA extraction (data shown in Fig. 9). Protocols were adopted as Taylor et al.[54] described. A model mixture of DNA and protein was used to test the DNA-extracting capability of modified MNPs. The recovery yields and purities of DNA isolated by magnetic particles of various functional groups were determined by yield and ratio of A_{260} to A_{280}. Commonly, A_{260}/A_{280} ratio at 1.7–2.0 is considered of high purity.

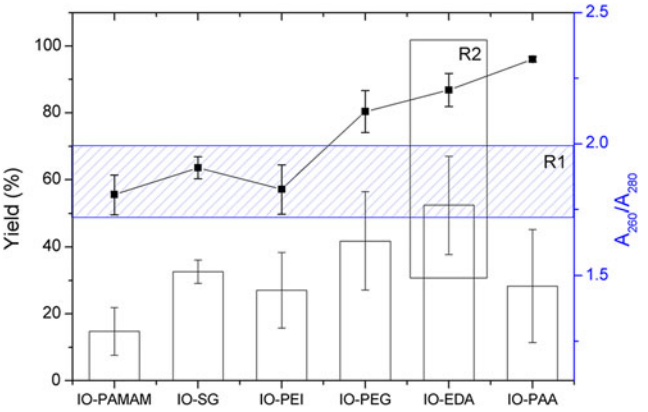


FIG. 9. Recovery yields and purities of DNA samples extracted with different magnetic particles: R1 region stands for the best A_{260}/A_{280} ratio of pure DNA; R2 region shows that IO-EDA has the best yield and the suitable ratio of A_{260}/A_{280} among those hydrophilic superparamagnetic iron oxide nanoparticles.

As can be seen from Fig. 8, in terms of both recovery yield (higher than 80%) and purity (A_{260}/A_{280} = 1.7–2.0, as the shadow zone marked), IO-EDA was unambiguously the best candidate (marked with R2 in a rectangle). The second best is IO-PEG. All the others lack of enough recovery yield or selectivity, or both. This indicated that the type and amount of surface functional groups both had significant effects on the recovery yield and purity of isolated DNA.

It had been expected that the positively charged amino- and imine-containing macromolecules functionalized magnetic nanoparticles (IO-PEI and IO-PAMAM) could have reasonable recovery yield by electronic static attraction because DNA is negatively charged. However, the very low yield and selectivity suggested that the charge did not play a dominant role. Possibly, only aminos work for selective adsorption, but these two mostly contain imine groups. The relative large steric hindrance of imine in macromolecules makes it hard to form hydrogen bonds.

https://doi.org/10.1557/jmr.2012.35 Published online by Cambridge University Press

Surprisingly, negatively charged IO-SG and IO-PAA had better performance, suggesting the carboxyl groups have some specific interaction with DNA, possibly by hydrogen bonds. PAA even showed the highest recovery yield, which should relate to its far higher organic molecules mass loading ratio than other nanoparticles, as revealed by TGA (Fig. 8). But, the relatively low selectivity suggested their wide but nonspecific interactions with DNA and protein.

The surface of IO-EDA magnetic particles contain mostly $–NH_2$ groups, which made the particles positively charged. TGA data showed the relative high loading of modifactory molecules onto the surface of MNPs (4.3%, higher than PEI and PEG). They could interact with DNA in a more specific way, associated with electrostatic pull,[55] which lead to much better recovery yield and purity. IO-PEG also got reasonable yield and the ratio of A_{260} to A_{280}, though the mass loading is quite low. This is due to the capability of PEG to transfer DNA from B-type to A-type.[54] Such results confirmed the former reports that ways of DNA binding onto modified magnetic particles are through electrostatic pull[55] or absorption onto the modified iron oxide nanoparticles in high salt solution.[54]

IV. CONCLUSION

In summary, a facile one-pot solvothermal method by introducing various tuning reagents was developed to prepare surface-modified magnetite nanoparticles with tunable magnetism, sizes, suspension stability, and surface charge. These hydrophilic magnetite nanoparticles are evidenced excellent candidates for bioseparation by selectively extracting DNA molecules from a model of cell fractures. Results indicated that PEG and amino-containing organic modules can benefit from the selective extraction of DNA molecules, which should be inspirative for further designing such magnetic nanoparticles for bioapplications.

ACKNOWLEDGMENTS

This work was supported by National Natural Science Foundation of China, the Foundation for Authors of National Excellent Doctoral Dissertations of People's Republic of China, the Program for New Century Excellent Talents in Universities, the 973 Program (2011CBA00503, 2011CB932403), the National Transgenic Major Program (2008ZX08012-001), and the Fundamental Research Funds for the Central Universities.

REFERENCES

1. S.J. Son, J. Reichel, B. He, M. Schuchman, and S.B. Lee: Magnetic nanotubes for magnetic-field-assisted bioseparation, biointeraction, and drug delivery. *J. Am. Chem. Soc.* **127**(20), 7316 (2005).
2. W. Fang, X. Chen, and N. Zheng: Superparamagnetic core-shell polymer particles for efficient purification of his-tagged proteins. *J. Mater. Chem.* **20**(39), 8624 (2010).
3. J. Chun, S.W. Seo, G.Y. Jung, and J. Lee: Easy access to efficient magnetically recyclable separation of histidine-tagged proteins using superparamagnetic nickel ferrite nanoparticle clusters. *J. Mater. Chem.* **21**(18), 6713 (2011).
4. A-H. Lu, E.L. Salabas, and F. Schüth: Magnetic nanoparticles: Synthesis, protection, functionalization, and application. *Angew. Chem. Int. Ed.* **46**(8), 1222 (2007).
5. S. Berensmeier: Magnetic particles for the separation and purification of nucleic acids. *Appl. Microbiol. Biotechnol.* **73**(3), 495 (2006).
6. R. Xu, G. Sun, Q. Li, E. Wang, and J. Gu: A dual-responsive superparamagnetic Fe_3O_4/Silica/PAH/PSS material used for controlled release of chemotherapeutic agent, keggin polyoxotungstate, PM-19. *Solid State Sci.* **12**, 1720 (2010).
7. D. Chen, M. Jiang, N. Li, H. Gu, Q. Xu, J. Ge, X. Xia, and J. Lu: Modification of magnetic silica/iron oxide nanocomposites with fluorescent polymethacrylic acid for cancer targeting and drug delivery. *J. Mater. Chem.* **20**(31), 6422 (2010).
8. Z. Xu, Y. Feng, X. Liu, M. Guan, C. Zhao, and H. Zhang: Synthesis and characterization of Fe_3O_4@SiO_2@poly-L-alanine, peptide brush-magnetic microspheres through NCA chemistry for drug delivery and enrichment of BSA. *Colloids Surf. B* **81**, 503 (2010).
9. B. Luo, S. Xu, A. Luo, W.R. Wang, S.L. Wang, J. Guo, Y. Lin, D.Y. Zhao, and C.C. Wang: Mesoporous biocompatible and acid-degradable magnetic colloidal nanocrystal clusters with sustainable stability and high hydrophobic drug loading capacity. *ACS Nano* **5**(2), 1428 (2011).
10. P. Govindaiah, T.J. Park, Y.J. Jung, S.J. Lee, D.Y. Ryu, J.H. Kim, and I.W. Cheong: Luminescent iron oxide nanoparticles prepared by one-pot aphen-functionalization. *Macromol. Res.* **18**(11), 1109 (2010).
11. M.M. Lin, S. Li, H.H. Kim, H. Kim, H.B. Lee, and M. Muhammed: Complete separation of magnetic nanoparticles via chemical cleavage of dextran by ethylenediamine for intracellular uptake. *J. Mater. Chem.* **20**(3), 444 (2009).
12. J. Liu, Z. Sun, Y. Deng, Y. Zou, C. Li, X. Guo, L. Xiong, Y. Gao, F. Li, and D. Zhao: Highly water-dispersible biocompatible magnetite particles with low cytotoxicity stabilized by citrate groups. *Angew. Chem. Int. Ed.* **121**(32), 5989 (2009).
13. J.K. Oh and J.M. Park: Iron oxide-based superparamagnetic polymeric nanomaterials: Design, preparation, and biomedical application. *Prog. Polym. Sci.* **36**, 168 (2011).
14. S. Xuan, F. Wang, J.M.Y. Lai, K.W.Y. Sham, Y.X.J. Wang, S.F. Lee, J.C. Yu, C.H.K. Cheng, and K.C.F. Leung: Synthesis of biocompatible, mesoporous Fe_3O_4 nano/microspheres with large surface area for magnetic resonance imaging and therapeutic applications. *ACS Appl. Mater. Interfaces* **3**, 237 (2011).
15. Z. Shi, K.G. Neoh, E.T. Kang, B. Shuter, S-C. Wang, C. Poh, and W. Wang: (Carboxymethyl)chitosan-modified superparamagnetic iron oxide nanoparticles for magnetic resonance imaging of stem cells. *ACS Appl. Mater. Interfaces* **1**(2), 328 (2008).
16. A.K. Gupta and S. Wells: Surface-modified superparamagnetic nanoparticles for drug delivery: Preparation, characterization, and cytotoxicity studies. *IEEE Trans. Nanobiosci.* **3**(1), 66 (2004).
17. A.K. Gupta and M. Gupta: Synthesis and surface engineering of iron oxide nanoparticles for biomedical applications. *Biomaterials* **26**(18), 3995 (2005).
18. G.M. da Costa, E. De Grave, P.M.A. de Bakker, and R.E. Vandenberghe: Synthesis and characterization of some iron oxides by sol-gel method. *J. Solid State Chem.* **113**(2), 405 (1994).
19. S.R. Dave and X. Gao: Monodisperse magnetic nanoparticles for biodetection, imaging, and drug delivery: A versatile and evolving technology. *Nanomed. Nanobiotechnol.* **1**(6), 583 (2009).
20. X. Teng and H. Yang: Synthesis of face-centered tetragonal FePt nanoparticles and granular films from Pt@Fe_2O_3 core-shell nanoparticles. *J. Am. Chem. Soc.* **125**(47), 14559 (2003).

https://doi.org/10.1557/jmr.2012.35 Published online by Cambridge University Press

21. J. Ge, Y. Hu, M. Biasini, W.P. Beyermann, and Y. Yin: Superparamagnetic magnetite colloidal nanocrystal clusters. *Angew. Chem. Int. Ed.* **46**(23), 4342 (2007).
22. L. Wang, J. Bao, L. Wang, F. Zhang, and Y. Li: One-pot synthesis and bioapplication of amine-functionalized magnetite nanoparticles and hollow nanospheres. *Chemistry* **12**(24), 6341 (2006).
23. B. Tang, G. Wang, L. Zhuo, J. Ge, and L. Cui: Facile route to α-FeOOH and α-Fe_2O_3 nanorods and magnetic property of γ-Fe_2O_3 nanorods. *Inorg. Chem.* **45**(13), 5196 (2006).
24. T. Taniguchi, K. Nakagawa, T. Watanabe, N. Matsushita, and M. Yoshimura: Hydrothermal growth of fatty acid stabilized iron oxide nanocrystals. *J. Phys. Chem. C* **113**(3), 839 (2008).
25. H. Deng, X. Li, Q. Peng, X. Wang, J. Chen, and Y. Li: Monodisperse magnetic single-crystal ferrite microspheres. *Angew. Chem. Int. Ed.* **117**(18), 2842 (2005).
26. J. Ge, Y. Hu, T. Zhang, and Y. Yin: Superparamagnetic composite colloids with anisotropic structures. *J. Am. Chem. Soc.* **129**(29), 8974 (2007).
27. Q. Yuan, R. Venkatasubramanian, S. Hein, and R.D.K. Misra: A stimulus-responsive magnetic nanoparticle drug carrier: Magnetite encapsulated by chitosan-grafted-copolymer. *Acta Biomater.* **4**(4), 1024 (2008).
28. X. Wang, L. Zhou, Y. Ma, X. Li, and H. Gu: Control of aggregate size of polyethyleneimine-coated magnetic nanoparticles for magnetofection. *Nano Res.* **2**(5), 365 (2009).
29. G-y. Li, K-l. Huang, Y-r. Jiang, P. Ding, and D-l. Yang: Preparation and characterization of carboxyl functionalization of chitosan derivative magnetic nanoparticles. *Biochem. Eng. J.* **40**(3), 408 (2008).
30. M. Mikhaylova, D.K. Kim, C.C. Berry, A. Zagorodni, M. Toprak, A.S.G. Curtis, and M. Muhammed: BSA immobilization on amine-functionalized superparamagnetic iron oxide nanoparticles. *Chem. Mater.* **16**(12), 2344 (2004).
31. P. Tartaj, T. Gonzalez-Carreno, A.F. Rebolledo, O. Bomati-Miguel, and C.J. Serna: Direct aerosol synthesis of carboxy-functionalized iron oxide colloids displaying reversible magnetic behavior. *J. Colloid Interface Sci.* **309**(1), 68 (2007).
32. A. Yourdkhani and G. Caruntu: Highly ordered transition metal ferrite nanotube arrays synthesized by template-assisted liquid phase deposition. *J. Mater. Chem.* **21**(20), 7145 (2011).
33. X. Yu, Y. Shan, B. Du, and K. Chen: One-pot and template-free fabrication of dendritic and octahedral single-crystal magnetites. *CrystEngComm.* **13**, 1525 (2011).
34. J. Liang, L. Li, M. Luo, and Y. Wang: Fabrication of Fe_3O_4 octahedra by a triethanolamine-assisted hydrothermal process. *Cryst. Res. Technol.* **46**(1), 95 (2011).
35. X. Wang, Z. Zhao, J. Qu, Z. Wang, and J. Qiu: Shape-control and characterization of magnetite prepared via a one-step solvothermal route. *Cryst. Growth Des.* **10**, 2863 (2010).
36. W. Cheng, K. Tang, and J. Sheng: Highly water-soluble superparamagnetic ferrite colloidal spheres with tunable composition and size. *Chem. Eur. J.* **16**(12), 3608 (2010).
37. H. Sun, H. Wei, H. Zhang, Y. Ning, Y. Tang, F. Zhai, and B. Yang: Self-assembly of CdTe nanoparticles into dendrite structure: A microsensor to Hg^{2+}. *Langmuir* **27**(3), 1136 (2011).
38. Y. Li, C. Dong, J. Chu, J. Qi, and X. Li: Surface molecular imprinting onto fluorescein-coated magnetic nanoparticles via reversible addition fragmentation chain transfer polymerization: A facile three-in-one system for recognition and separation of endocrine disrupting chemicals. *Nanoscale* **3**, 280 (2011).
39. W.H. Zhou, C.H. Lu, X.C. Guo, F.R. Chen, H.H. Yang, and X.R. Wang: Mussel-inspired molecularly imprinted polymer coating superparamagnetic nanoparticles for protein recognition. *J. Mater. Chem.* **20**(5), 880 (2009).
40. X. Song, Y. Yang, J. Liu, and H. Zhao: PS colloidal particles stabilized by graphene oxide. *Langmuir* **27**(3), 1186 (2011).
41. C. Wang, S. Tao, W. Wei, C. Meng, F. Liu, and M. Han: Multifunctional mesoporous material for detection, adsorption and removal of Hg^{2+} in aqueous solution. *J. Mater. Chem.* **20**(22), 4635 (2010).
42. H. Chen, Y. Zhao, M. Yang, J. He, P.K. Chu, J. Zhang, and S. Wu: Glycine-assisted hydrothermal synthesis of peculiar porous alpha-Fe_2O_3 nanospheres with excellent gas-sensing properties. *Anal. Chim. Acta* **659**(1–2), 266 (2010).
43. K. Zhou, Y. Zhu, X. Yang, and C. Li: One-pot preparation of graphene/Fe3O4 composites by a solvothermal reaction. *N. J. Chem.* **34**(12), 2950 (2010).
44. D.A. Tomalia, H. Baker, J. Dewald, M. Hall, G. Kallos, S. Martin, J. Roeck, J. Ryder, and P. Smith: A new class of polymers: Starburst-dendritic macromolecules. *Polym. J.* **17**(1), 117 (1985).
45. D.A. Tomalia, H. Baker, J. Dewald, M. Hall, G. Kallos, S. Martin, J. Roeck, J. Ryder, and P. Smith: Dendritic macromolecules: Synthesis of starburst dendrimers. *Macromolecules* **19**(9), 2466 (1986).
46. Z. Zhang, Y. Cui, and Q. Wan: Surface modification of magnetic silica microspheres and its application to the isolation of plant genomic nucleic acids. *Chin. J. Anal. Chem.* **35**(1), 31 (2007).
47. A.G. Roca, J.F. Marco, M.P. Morales, and C.J. Serna: Effect of nature and particle size on properties of uniform magnetite and maghemite nanoparticles. *J. Phys. Chem. C* **111**(50), 18577 (2007).
48. S. Wan, J. Huang, H. Yan, and K. Liu: Size-controlled preparation of magnetite nanoparticles in the presence of graft copolymers. *J. Mater. Chem.* **16**(3), 298 (2006).
49. L.B. Hoch, E.J. Mack, B.W. Hydutsky, J.M. Hershman, J.M. Skluzacek, and T.E. Mallouk: Carbothermal synthesis of carbon-supported nanoscale zero-valent iron particles for the remediation of hexavalent chromium. *Environ. Sci. Technol.* **42**(7), 2600 (2008).
50. J. Zhi, Y. Wang, Y. Lu, J. Ma, and G. Luo: In situ preparation of magnetic chitosan/Fe3O4 composite nanoparticles in tiny pools of water-in-oil microemulsion. *React. Funct. Polym.* **66**(12), 1552 (2006).
51. S.H. Wang, X. Shi, M. Van Antwerp, Z. Cao, S.D. Swanson, X. Bi, and J.R. Baker, Jr.: Dendrimer-functionalized iron oxide nanoparticles for specific targeting and imaging of cancer cells. *Adv. Funct. Mater.* **17**(16), 3043 (2007).
52. R. Narain, M. Gonzales, A.S. Hoffman, P.S. Stayton, and K.M. Krishnan: Synthesis of monodisperse biotinylated p (NIPAAm)-coated iron oxide magnetic nanoparticles and their bioconjugation to streptavidin. *Langmuir* **23**(11), 6299 (2007).
53. S. McBain, H. Yiu, A. El Haj, and J. Dobson: Polyethyleneimine functionalized iron oxide nanoparticles as agents for DNA delivery and transfection. *J. Mater. Chem.* **17**(24), 2561 (2007).
54. J.I. Taylor, C.D. Hurst, M.J. Davies, N. Sachsinger, and I.J. Bruce: Application of magnetite and silica-magnetite composites to the isolation of genomic DNA. *J. Chromatogr. A* **890**(1), 159 (2000).
55. B. Yoza, M. Matsumoto, and T. Matsunaga: DNA extraction using modified bacterial magnetic particles in the presence of amino silane compound. *J. Biotechnol.* **94**(3), 217 (2002).

https://doi.org/10.1557/jmr.2012.35 Published online by Cambridge University Press